Vol. 51: 183–201, 2023
https://doi.org/10.3354/esr01254

ENDANGERED SPECIES RESEARCH
Endang Species Res

Published July 6

Spatial segregation between phenotypes of the diablotin black-capped petrel *Pterodroma hasitata* during the non-breeding period

Yvan G. Satgé[1,2,*], Bradford S. Keitt[3], Chris P. Gaskin[4], J. Brian Patteson[5], Patrick G. R. Jodice[1,6]

[1]Department of Forestry and Environmental Conservation, Clemson University, Clemson, SC 29634, USA
[2]South Carolina Cooperative Fish and Wildlife Research Unit, Clemson, SC 29634, USA
[3]American Bird Conservancy, Santa Cruz, CA 95060, USA
[4]Northern New Zealand Seabird Trust, Auckland, 0985, New Zealand
[5]Seabirding Pelagic Trips, Hatteras, NC 27943, USA
[6]US Geological Survey South Carolina Cooperative Fish and Wildlife Research Unit, Clemson, SC 29634, USA

ABSTRACT: Despite growing support for ecosystem-based approaches, conservation is mostly implemented at the species level. However, genetic differentiation exists within this taxonomic level, putting genetically distinct populations at risk of local extinction. In the diablotin black-capped petrel *Pterodroma hasitata*, an endangered gadfly petrel endemic to the Caribbean, 2 phenotypes have been described: a smaller dark form and a heavier light form, which are genetically distinct. To assess possible differences in the marine distributions of phenotypes, in May 2019, we captured 5 adult black-capped petrels of each phenotype at sea in the western North Atlantic and equipped them with satellite transmitters. We used generalized linear mixed models to test the importance of phenotype on geographic distribution. Using kernel density estimations, we located use areas, quantified spatial overlap between forms, and assessed form-specific exposure to marine threats. Petrels were tracked for 11 to 255 d (mean ± SD: 102.1 ± 74.2 d). During the non-breeding period, all individuals ranged from 28.4 to 43.0° latitude. Phenotypes had significantly distinct non-breeding distributions, independent of time of year. The dark form used waters of the Carolinian marine ecoregion, and the light form used pelagic waters of the Virginian ecoregion, to the north. The dark form was more exposed to marine threats than the light form, in particular to mercury, microplastics, and marine traffic. The light form overlapped with proposed wind energy areas off the central US coast. These differences in exposure suggest possible differences in vulnerability, which can have repercussions on the viability of this imperiled species.

KEY WORDS: Distribution · Phenotype · Seabird · Threat exposure · Conservation

1. INTRODUCTION

Identifying behavioral and ecological traits of endangered species, such as seasonal distributions, migration patterns, habitat use, or trophic niche space, is critical to inform and prioritize conservation actions. These traits can act as ultimate drivers of and/or become consequences of genetic differentiation among populations (Bridle et al. 2004, Hellberg 2009, Ribeiro et al. 2012, Ryan et al. 2014, Friesen 2015, Lombal et al. 2020, Mancilla-Morales et al. 2020). In species that exhibit strong genetic differentiation, a limited understanding of behavioral and ecological traits and a subsequent lack of conserva-

*Corresponding author: ysatge@g.clemson.edu

Publisher: Inter-Research · www.int-res.com

tion actions focused at the population level could lead, either directly or indirectly, to reductions in population sizes or even to the loss of entire populations (Gaston 2001, but see Ennos et al. 2005, Winker 2010, Danckwerts et al. 2021). To effectively inform conservation, trait-based assessments of vulnerability require a proximate understanding of a population's sensitivity (the degree to which it is affected by a stressor), adaptive capacity (its ability to adapt to or recover from a stressor), and exposure (Butt et al. 2022). Therefore, understanding the spatial scales at which ecological and behavioral traits might vary, and at which threats may affect populations, has direct implications for conserving representation (the existence of genetic and phenotypic diversity) and redundancy (the capacity to persist despite the loss of a population) within a species.

Seabirds are highly vagile animals that are geographically constrained to a limited number of terrestrial nesting areas (e.g. oceanic islands or coastal areas) during the breeding season but often migrate to different marine ecoregions or even different ocean basins during the non-breeding season (Croxall et al. 2005, Shaffer et al. 2006, Alerstam et al. 2019). Therefore, seabirds experience exposure to marine threats (including but not limited to fisheries bycatch, overfishing, pollution, and attraction to and collisions with ships and structures; Ronconi et al. 2015, Dias et al. 2019) across a wide geographic footprint. Due to the remote nature of their distribution, our ability to assess the exposure of seabirds to threats is often limited to calculating the spatiotemporal overlap between a population and the threats impacting it (Pereira et al. 2021, Fischer et al. 2021). Although this macro-scale exposure (Burger et al. 2011) does not necessarily imply interaction with marine threats, it is often used as a reasonable proxy for potential exposure (Le Bot et al. 2018).

Historically, the marine distribution of seabirds was assessed through systematic at-sea surveys and opportunistic day trips. While highly informative, these surveys are often limited in geographic scope, do not distinguish characteristics of individuals observed, such as phenotype, sex, or breeding status, and do not provide information on connectivity among oceanic basins or between breeding sites and marine areas (Carroll et al. 2019). In contrast, tracking individuals does allow for the collection of the aforementioned data and, therefore, also allows for the opportunity to investigate potential drivers of genetic differentiation and threats affecting populations. Nevertheless, the extent of available tracking data in terms of species tracked, populations tracked within species, and sample sizes within tracking studies is often limited for many species that are globally threatened or endangered (Bernard et al. 2021) or that are geopolitically biased in the location of breeding sites (e.g. fewer studies of tropical vs. temperate species; Mott & Clarke 2018).

The diablotin, or black-capped petrel *Pterodroma hasitata*, is an endangered gadfly petrel endemic to the Caribbean and occurs in waters of the western North Atlantic Ocean, Caribbean Sea, and Gulf of Mexico (Simons et al. 2013, Jodice et al. 2015, 2021). With a global population estimated at 2000–4000 individuals (BirdLife International 2023), the species is considered Endangered throughout its range (BirdLife International 2018) and is being considered by the US Fish and Wildlife Service for listing as threatened under the US Endangered Species Act (US Fish and Wildlife Service 2018). Known breeding populations are fragmented into 5 distinct breeding areas on the island of Hispaniola (although breeding is suspected in Dominica and Cuba; Wheeler et al. 2021).

Two color forms have been described (dark and light, with intermediate phenotypes) that differ in size, mass, and the amount of white plumage on the face, back of the neck, and underwing feathers (Howell & Patteson 2008) (Fig. S1 in the Supplement at www.int-res.com/articles/suppl/n051p183_supp.pdf). The species has a fixed population structure (assessed by the number and proportion of fixed mutations in haplotypes; Manly et al. 2013) and strong genetic divergence between the 2 forms, with light and intermediate forms belonging to a unit separate from the dark form (Manly et al. 2013). Allopatric and temporal reproductive isolation has been described as the most probable mechanism for genetic differentiation (Haney 1987, Manly et al. 2013). For example, the dark form breeds at all 5 sites, but the light form is known to breed only at one, in the central Dominican Republic (E. Rupp pers. comm.). Analysis of molt patterns and data from remote cameras suggests that the light form breeds from early October to late April, while the dark form breeds from mid-November to mid-June (Howell & Patteson 2008, Manly et al. 2013, E. Rupp pers. comm.). At sea, observations obtained primarily from ship-based surveys suggest that both forms use similar areas during the non-breeding season (Howell & Patteson 2008, Simons et al. 2013), and that differences in foraging strategies do not appear to occur (see Haney 1987). However, pelagic observations in other areas of the species' Atlantic range have become increasingly available in the last decade and suggest that dark individuals are more com-

monly observed in the south and light individuals in the north (eBird 2022).

This apparent dual distribution may subject each form of the black-capped petrel to different levels of exposure to marine threats, further complicating conservation planning. For example, black-capped petrels show high levels of mercury bioaccumulation (Simons et al. 2013, Y. Satgé unpubl. data, K. Sutherland unpubl. data), which may have both individual- and population-level consequences (Tartu et al. 2013, Goutte et al. 2014, Bond et al. 2015). Petrels are also expected to be affected by marine microplastics (Dias et al. 2019) due to their diet and limited capacity to regurgitate plastic fragments (Furness 1985, Moser & Lee 1992, Rodríguez et al. 2019). *Pterodroma* petrels are considered to be less susceptible to fisheries bycatch than larger pelagic species (Waugh et al. 2012) but they are not immune to it (Richard et al. 2017, Parker & Rexer-Huber 2019, Rexer-Huber & Parker 2019). Although black-capped petrels have yet to be reported as bycatch in the western North Atlantic (Li et al. 2016), they may still be at risk of bycatch in pelagic longline fisheries (Zhou et al. 2019). Furthermore, black-capped petrels scavenge on chum and discards, which may expose them to collisions with cables used in trawl fisheries (including net-sonde cables, which are still used in the region), a type of bycatch that is often overlooked by on-board observers (Debski & Pierre 2014). In addition to fishing vessels, shipping (which includes cargo, tankers, and cruise ships) can have adverse effects on petrels through attraction to and collision with lighted vessels (Glass & Ryan 2013, Ryan et al. 2021, Copsey 2022), pollution (Heubeck et al. 2003, Fox et al. 2016, King et al. 2021), and displacement (Lieske et al. 2020). Finally, petrels may be adversely affected by marine energy activities, including petroleum exploration and extraction as well as offshore wind energy development and production. Petrels are susceptible to light attraction (from production platforms, construction and support vessels, and gas flaring; Ronconi et al. 2015, Fraser & Carter 2018), contaminants (accidental oil spills and regular discharge of produced waters, through contact or bioaccumulation; Fraser et al. 2006, Ronconi et al. 2015, Jodice et al. 2021), and displacement. In the US Central Atlantic, the black-capped petrel is the avian species with the highest population sensitivity to offshore wind facilities and has a high sensitivity to collision and displacement (Robinson Willmott et al. 2013).

Given its small population size and its exposure to substantial threats at breeding sites (Wheeler et al. 2021), even low levels of adult mortality resulting from these marine threats can adversely affect the viability of the species. Therefore, in the spring of 2019, we attempted to assess the distribution of both phenotypes of black-capped petrel using satellite telemetry on individuals captured at sea. The objectives of this study were to (1) evaluate differences in the non-breeding distributions of both forms and (2) assess macro-scale exposure to marine threats in both forms. As a first step towards assessing the species' vulnerability to marine threats, a better understanding of how the phenotypes use the marine environment will elucidate possible differences in ecological niches and their roles in driving black-capped petrel exposure. In addition, given increased interest in the production of marine renewable energy in the pelagic environment off the eastern USA, the results of this study will help inform planning decisions that take into account the conservation of this endangered species.

2. MATERIALS AND METHODS

2.1. Fieldwork

At-sea captures occurred during May 2019 in Gulf Stream waters, ~60 km southeast of Cape Hatteras, North Carolina, USA, an area where foraging black-capped petrels are commonly found during the non-breeding season (Simons et al. 2013, Jodice et al. 2015) (Fig. 1). We chose to capture birds during the northern spring because individuals of the light form of black-capped petrel appear to be more common off Hatteras at this time of year, whereas dark-form petrels appear to be more common during the late summer and fall (Howell & Patteson 2008). After sunrise, we located black-capped petrels from a ~20 m research vessel with the aid of chumming (a mixture of fish meal and shark liver oil). Upon detection of petrels, we deployed a metal cage (~20 × 20 × 40 cm) that was secured to a drifting vinyl mooring buoy and contained blocks of frozen chum, and launched a ~3 m motorized inflatable boat with 2 occupants: a pilot and a catcher. We positioned the inflatable boat upwind from the buoy, keeping the bow of the boat and the catcher facing downwind. We attempted to capture black-capped petrels that had flown upwind along the oil slick and approached within 10–15 m forward of the bow. We used a modified air-propelled whale tagger (ARTS Whale Tagger), custom-fitted to launch 4 narrow PVC tubes (approx. 50 × 1.5 cm diameter; designed to float) attached to the corners of a 4 × 4 m mist net (adapted from Rayner et al. 2020). The net launcher was powered by compressed air

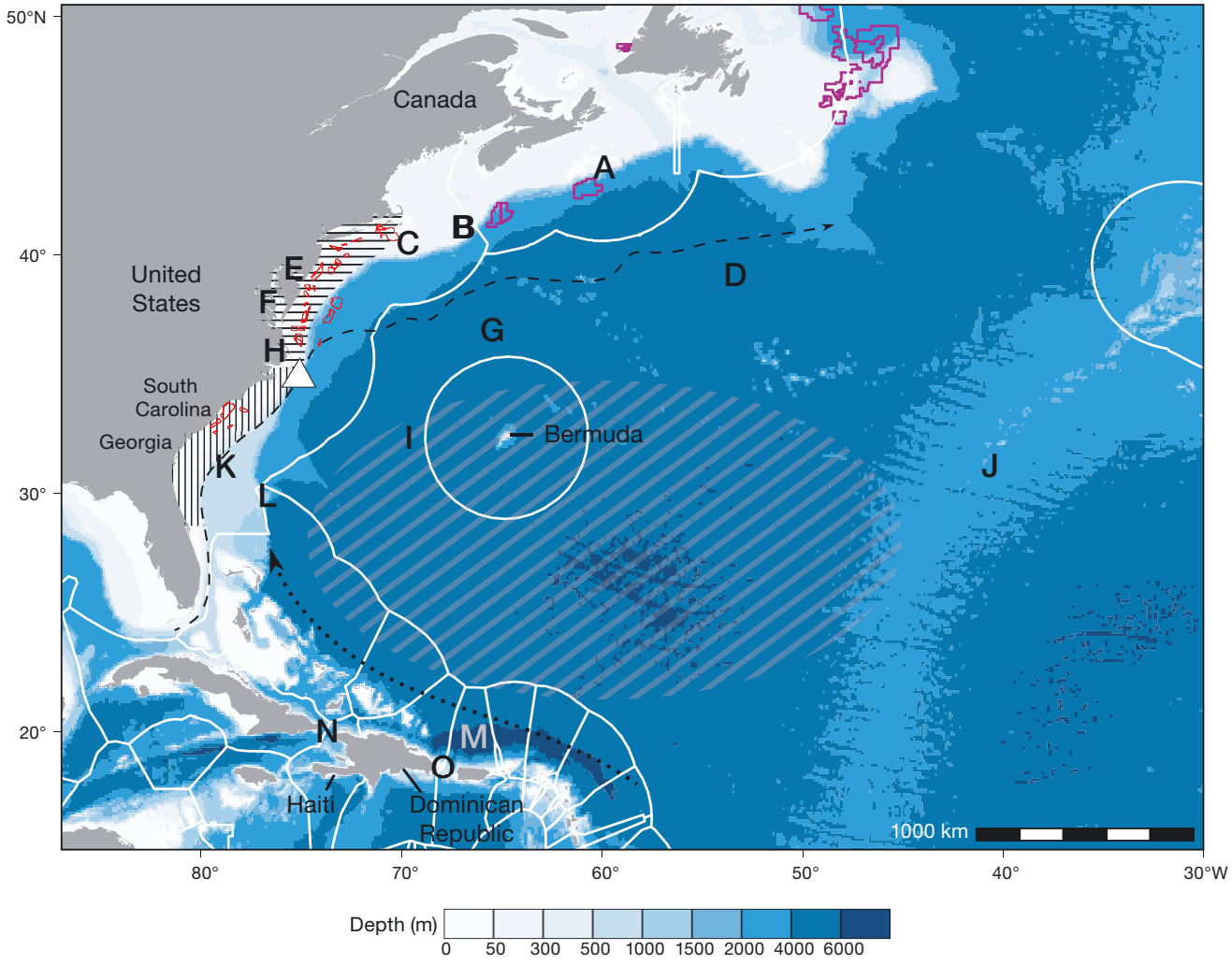

Fig. 1. Study area. White triangle: capture location. Letters indicate geographic and oceanographic features. A: Banquereau Bank; B: Georges Bank; C: Nantucket Shoals; D: Sohm Plains; E: Delaware Bay; F: Chesapeake Bay; G: Caryn Seamount; H: Cape Hatteras; I: Hatteras Plains; J: Mid-Atlantic Ridge; K: Charleston Bump; L: Blake Spur; M: Puerto Rico Trench; N: Windward Passage; O: Mona Passage. Black lines: general location of the western edge of the Gulf Stream (dashed) and the Antilles Current (dotted). Horizontal hatching: the Middle Atlantic Bight; vertical hatching: South Atlantic Bight; grey hatched area: general extent of the Sargasso Sea. White polygons: exclusive economic zones. Purple polygons: petroleum leases; red polygons: offshore wind leases. Black-capped petrels have been confirmed to nest in Haiti and the Dominican Republic

from a dive tank. Upon capture, we transferred petrels to the research vessel for processing and transmitter deployment. This transfer lasted <3 min.

After assessing captured petrels for general condition, we measured body mass (±5 g), tarsus (±0.1 mm), wing cord (±1 mm), exposed culmen length (±0.1 mm), and bill depth at gonys (±0.1 mm). We banded petrels with individually numbered metal bands (US Geological Survey [USGS] Bird Banding Laboratory). We collected a few drops of blood from one metatarsal vein for genetic sexing. We photographed the birds' profiles and upper- and underwings and classified them as dark, intermediate, or light forms. In addition, we assessed the age classes of the birds based on the shape and aspect of secondary flight feathers: we assumed that first-year juveniles had pointy feathers with a uniform aspect (due to limited wear and uniform growth), and immatures (1–4 yr) and adults had worn secondaries with a varied aspect (due to scattered molting of flight feathers) (K. Sutherland pers. comm.). Finally, we recorded any molting of flight feathers. We used a *t*-test to compare each morphometric measurement between forms (for all statistical analyses, we grouped light and intermediate forms following Manly et al. 2013).

We deployed solar-powered platform terminal transmitters (PTTs) (GT-5GS, GeoTrak, 5 g, n = 8; 5g-Solar-PTT, Microwave Telemetry, 5 g, n = 2) on

petrels whose body mass was >350 g. For the GeoTrak PTTs, we chose a duty cycle of 6 h on, 28 h off to benefit from the most extensive tracking time while optimizing battery usage; Microwave Telemetry PTTs had a pre-set duty cycle of 5 h on, 48 h off. All PTTs were custom-fitted with a base of marine-grade epoxy ~2 mm in thickness, in which 4 tubular channels were made perpendicular to the length of the PTT. Customized PTTs weighed 8.5 g (≤2.5% of body mass of the lightest petrel in Simons et al. 2013, Jodice et al. 2015, and Satgé et al. 2019). We deployed PTTs dorsally between the wings and centered above the vertebrae, using 4 subcutaneous sutures and a small amount of glue (sensu Jodice et al. 2015). Before release, we placed equipped birds in a holding crate lined with a dry cloth towel until chest feathers were preened (~20 min).

Molecular sexing was performed at the Centro de Ecologia, Evolução e Alterações Ambientais, University of Lisbon, Portugal, following Fridolfsson & Ellegren (1999) with primers 2550F and 2718R. All animal handling was performed under Clemson University's Animal Care and Use protocol AUP2019-033. Banding and PTT deployment were authorized by the USGS Bird Banding Lab (permit #22408).

2.2. Spatial analysis of tracks

Tracking data were imported to Movebank (https://www.movebank.org) via Service Argos. Argos applies a Kalman Filter model and provides error statistics and a quality class (3, 2, 1, 0, B, A, Z, in decreasing order of quality) for each estimated location. To improve the accuracy of Argos location estimates, we filtered locations and estimated the most probable 'true' location using a continuous-time random walk state-space model (package 'foieGras' in R; Jonsen et al. 2019). The mean duration between 2 consecutive Argos locations was 32 min; therefore, we used a time-step parameter of 30 min; we also included a maximum flight speed of 20 m s^{-1} as a model parameter. Fitting algorithms can estimate locations during periods when PTTs are off but the precision of fitted locations decreases during long periods without transmissions, and unrealistic estimations may occur. Therefore, instead of filtering fitted locations to an arbitrary time period (e.g. 1–2 h from first or last Argos location during an 'on' period), we selected fitted locations in on and off periods based on their spatial standard errors. Hence, we kept only fitted locations where the standard error for longitude and latitude was less than the 95th percentile of the error radius of location classes 0–3 (10.3 km; Table S1).

We restricted analysis of location data to a period of time during which most birds were tracked, removing data from individuals tracked for less than 20 d (n = 3). On 18 July, a single individual started traveling eastward towards the mid-Atlantic ridge until 1 August, at which point the PTT stopped transmitting (see Figs. 2 & S2). This behavior is consistent with vagrancy observed in black-capped petrels (Simons et al. 2013); therefore, we considered these locations as outliers (they accounted for 1.3% of the total number of locations). This filtering resulted in a study time frame of 14 May to 25 August 2019, which encompassed 70% of all locations and included 7 individual birds (dark: n = 3; light: n = 4). After determining that the distributions of latitude and longitude in each phenotype were not normally distributed (Shapiro-Wilk normality test with $p < 0.005$ for both groups), we compared longitudinal and latitudinal distributions between dark and light forms using Wilcoxon rank sum tests. We estimated the magnitude of difference between groups by calculating Cohen's *d* effect size (function 'cohen.d' in package 'effsize' in R; Torchiano 2020). Cohen's *d* is defined as the difference between 2 means divided by a standard deviation for the data. Cohen (1988) suggested quantitative descriptors as follows: $d \leq 0.2$ represents a small effect, $0.2 < d \leq 0.5$ a moderate effect, and $d > 0.5$ a large effect (but see Sawilowsky 2009 for a discussion of descriptors). Because of the imbalanced number of individuals of each sex (n = 2 females and n = 5 males), we did not assess the effect of sex on petrel distribution.

The use of foraging areas may also depend on the time of year, an individual's phenology, or on individual variability. Marine spatial data in the western North Atlantic is inherently constrained by the continental coastline of the eastern USA (roughly a southwest-to-northeast diagonal; Fig. 1), and the distributions of latitude and longitude in black-capped petrel data were non-parametric. Therefore, to compare latitudinal and longitudinal distributions with phenotype, we used generalized linear mixed models with a gamma distribution and inverse link, and included date and individual as random effects (function 'glm' in package 'stats' in R). The number of locations per tracked day per individual ranged from 1–17 (mean: 5.9). To avoid any variations within individuals within dates, we used the latitude and longitude of the mean daily location for each individual. We did not include longitude as a fixed effect in the model of latitude nor did we include latitude as a fixed effect in

the model of longitude because latitude and longitude were correlated (Spearman's correlation index $\rho = 0.72$, $p < 0.005$). We estimated the importance of phenotype as the absolute value of the *t*-statistic for each model (package 'caret' in R; Kuhn et al. 2020).

We calculated utilization distributions (UDs) for both phenotypes using kernel density estimations in package 'adehabitat' in R (Calenge 2006; with smoothing parameter $h = 0.3$ and grid = 1000). We chose the smoothing parameter through successive trials and retained a value that conserved sufficient details in distribution patterns to locate high-use areas without excessive smoothing. Within a form, all individuals were grouped. We estimated the amount of spatial overlap among home range (90% UD) and core (50% UD) areas between the 2 forms. We also quantified the extent of spatial overlap in the home range and core areas of both forms using Bhattacharyya's affinity (BA). BA is a function of the product of the UDs of 2 populations (here dark and light forms) that assumes each population uses space independently from the other (Fieberg & Kochanny 2005). A BA value = 0 indicates no overlap while a BA value = 1 indicates complete overlap. Finally, we estimated overlap of the 2 populations with exclusive economic zones (EEZs; VLIZ 2019) and marine ecoregions (Spalding et al. 2007) by calculating the proportion of the 50 and 90% UDs of each phenotype within EEZs and international waters, and ecoregions and high seas, respectively.

2.3. Overlap with habitat features and marine-based threats

The black-capped petrel is considered to be strongly associated with the Gulf Stream off the southeast coast of the USA (Haney 1987, Jodice et al. 2015, Winship et al. 2018), so we examined differences between dark and light forms of black-capped petrels in their use of 2 key habitat features: ocean depth and sea surface temperature (SST). We did so by calculating spatial statistics for ocean depth (raster ETOPO1; 1 arc-minute; Amante & Eakins 2009) and SST (raster HYCOM; 0.08 arc-degree; May–September 2019; Cummings & Smedstad 2013) for all raster cells overlapping with 50 and 90% UDs of each form. We also compared differences in the distributions of environmental values (i.e. the depth and SST raster values extracted from all cells overlapping UDs) between phenotypes using Wilcoxon rank sum tests.

We then sought to quantify differences between dark and light forms of black-capped petrels in terms of their macro-exposure to marine-based threats in the western North Atlantic. We defined macro-scale exposure as the level of occurrence of a threat within the home range and core areas of each phenotype, sensu Burger et al. (2011) and Waggitt & Scott (2014). We included assessments of mercury, plastics, fisheries, shipping, and marine energy. We assessed the potential exposure of black-capped petrels to mercury using, as a proxy, a raster file of modeled total present-day mercury concentrations in the mixed layer (i.e. from the ocean surface to 50 m depth; Fig. 3a in Zhang et al. 2014) with a resolution of 1 × 1° (between 80 × 100 and 100 × 122 km, depending on latitude). We quantified potential exposure to plastics using, as a proxy, global models of the spatial distribution of microplastics (van Sebille et al. 2015). To quantify potential exposure to plastics, we averaged concentrations of microplastics (g km^{-2}) predicted by the Maximenko, Lebreton, and van Sebille models at the original 1 × 1° scale (Fig. 3 in van Sebille et al. 2015). We obtained data on daily commercial fishing effort from Global Fishing Watch (http://globalfishingwatch.org/; accessed 1 July 2021). By combining satellite tracking of commercial fishing vessels equipped with automatic identification systems and convolutional neural networks, the activity of >70 000 vessels larger than 15 m (>50–70% of the global fishing effort) is categorized as fishing or not fishing (Kroodsma et al. 2018). We summed all available daily effort data from May to August 2019 at 0.1° cell resolution (between 8 × 9.5 and 10 × 12.5 km depending on latitude). To assess overlap with marine traffic, we used a data set of annual vessel transit counts collected from automatic identification systems (where a single transit count corresponds to each time a vessel track passes through, starts, or stops within a 100 m grid cell) provided by the US Office for Coastal Management (2021). We aggregated raster data attributed to cargo, tanker, and all other vessel types (which includes fishing, passenger, pleasure craft and sailing, and tug and towing), for 2017 (the latest available year) at a resolution of 10 × 10 km. We obtained spatial data sets of active oil and gas exploration areas from the Canada–Nova Scotia Offshore Petroleum Board (https://www.cnsopb.ns.ca/resource-library/maps-and-coordinates; accessed 1 November 2021) and the Canada–Newfoundland and Labrador Offshore Petroleum Board (https://www.cnlopb.ca/information/shapefiles/; accessed 1 November 2021) and wind energy production data from the US Bureau of Ocean Energy Management (https://www.boem.gov/renewable-energy/mapping-and-data; accessed 22 March 2023). To simplify analyses, we merged individual lease plots occurring

within a US state and occurring in Newfoundland and Labrador (Canadian hydrocarbon areas) into project-scale lease areas (i.e. one lease area per administrative area). We also merged lease areas occurring in the US states of Rhode Island and Massachusetts into a single lease unit.

For each of the above attributes, we calculated spatial statistics from the values of all raster cells overlapping with 50 and 90% UDs: mean, minimum, maximum, standard deviation, and interquartile range (IQR). For fishing effort and ship transit, we also calculated the percentage of cells exposed to the threat as well as the sum of fishing effort and ship transit in both UDs. Shapiro-Wilk tests indicated that habitat features and threats followed non-parametric distributions; therefore, we assessed differences in the numeric distribution of threat values between phenotypes using Wilcoxon rank sum tests. We estimated the magnitude of the difference between groups by calculating Cohen's *d* effect size. We assessed exposure to marine energy production by calculating the proportion of the 50 and 90% UDs of each phenotype within the footprint of hydrocarbon and wind leases. We also calculated the number of individual petrels and individual tracking locations in lease areas along with the shortest distance between a tracking location and a lease area. For this descriptive analysis, we used data from the whole tracking period.

All statistical and spatial analyses were performed in R version 3.6.3 (R Core Team 2020). For all statistical analyses, we chose a significance level of $\alpha = 0.05$.

3. RESULTS

Capture attempts occurred on 8, 9, 11, and 14 May 2019 within a 25 km radius of 34.78° N, 75.33° W, along the continental slope of the eastern USA and the western edge of the Gulf Stream (Fig. 1). Capture effort ranged from 3.0–6.5 h on each of the 4 capture days. We captured 2 birds on 8 May, 4 birds on 9 May, 0 birds on 11 May, and 4 birds on 14 May. Sea state varied from Beaufort 2–5 among the 4 capture days (Fig. 1), with the lowest sea state occurring on 11 May when no birds were captured. Approximately 50% of capture attempts (i.e. nets launched) resulted in a successful capture. Sex (n = 3 females, n = 7 males) and morphometric data are summarized in Table 1. Of the 10 black-capped petrels we instrumented, we classified 5 birds as dark forms, 4 as light forms, and one as intermediate (Table 1). None of the petrels were first-year juveniles, but we could not assess age further and thus separate between immatures (1–4 yr) and adults (>4 yr; Simons et al. 2013). Morphometrics did not differ between sexes ($p > 0.05$ for all tests) (Table 1). Dark forms appeared smaller than light and intermediate forms in all metrics, but the differences were only

Table 1. Phenotype and morphometrics of black-capped petrels captured off Cape Hatteras, North Carolina, USA, May 2019. All molting feathers were in sheaths and growing. N: no molt was observed; P: primary flight feathers; S: secondary flight feathers. *significant difference ($p < 0.05$) between dark and light forms

Bird ID	Capture date	Sex	Mass (g)	Tarsus (mm)	Culmen (mm)	Bill depth (mm)	Wing cord (mm)	Molt
Dark forms								
469	8 May 2019	M	370	39.5	32.6	14.4	295	N
464	8 May 2019	F	390	38.7	32.5	13.7	292	N
466	9 May 2019	M	380	41.7	31.5	14.0	290	N
442	14 May 2019	M	380	39.2	34.8	13.6	280	N
441	14 May 2019	M	380	39.0	32.1	14.0	287	N
Average			380.0	39.6	32.7*	13.9	288.8*	
SD			6.32	1.07	1.12	0.28	5.11	
Light and intermediate forms								
468	9 May 2019	M	420	39.1	35.3	14.3	300	P1–2
462	9 May 2019	M	375	40.2	35.0	14.0	299	P3–4, S3
467[a]	9 May 2019	M	410	40.6	34.6	13.6	297	P2–4
465	14 May 2019	F	390	41.1	36.0	14.1	315	P2–3
463	14 May 2019	F	460	41.4	36.0	14.4	305	P1–2
Average			411.0	40.5	35.4*	14.1	303.2*	
SD			29.05	0.80	0.55	0.28	6.46	

[a]Intermediate form

Table 2. Summary of tracking period and geographic range of black-capped petrels tracked from May 2019–January 2020. Dates are given as yyyy-dd-mm. **Bold** lettering indicates dark phenotypes

Bird ID	First transmission date	Last transmission date	No. of tracking days	Latitudinal range (°N)	Longitudinal range (°W)	General areas used
469	2019-05-08	2019-05-25	17	30.3–35.8	80.2–74.5	South Atlantic Bight: continental shelf
464	2019-05-08	2019-08-25	109	29.4–38.5	78.2–70.3	Off Virginia: high seas
468	2019-05-09	2019-08-31	114	35.6–40.4	75.4–62.8	Off Delaware–New Jersey: high seas
466	2019-05-09	2019-05-20	11	31.5–37.4	78.9–72.8	South Atlantic Bight: continental shelf
462	2019-05-09	2019-11-14	189	17.4–43.1	75.9–56.3	Off Delaware–Connecticut: high seas; Dominican Republic
467	2019-05-09	2019-09-09	123	34.7–40.6	75.4–64.0	Off Virginia–New Jersey: high seas
442	2019-05-14	2020-01-24	255	17.3–38.0	80.1–64.1	Off South Carolina, North Carolina: continental slope; Haiti
441	2019-05-14	2019-08-30	108	30.4–38.2	79.3–65.8	Off Georgia–North Carolina: continental slope; off Virginia: high seas
465	2019-05-14	2019-08-01	79	31.1–39.8	77.2–50.5	Off Delaware, Maryland: high seas; mid-Atlantic
463	2019-05-14	2019-05-30	16	32.1–34.6	77.4–74.2	Off North Carolina: continental slope

significant for wing cord ($\bar{x}_{Dark(5)}$ = 289.3 mm vs. $\bar{x}_{Light(5)}$ = 303.2; $p < 0.05$; $t = -3.6$) and culmen length ($\bar{x}_{Dark(5)}$ = 32.5 mm vs. $\bar{x}_{Light(5)}$ = 35.4; $p < 0.05$; $t = -5.0$) (Table 1; $p > 0.05$ for all other comparisons). All light and intermediate forms were molting at least 2 flight feathers, but none of the dark forms were molting (Table 1). Deployed PTTs ranged from 1.85–2.30% of body mass (mean: 2.16%). Processing time ranged from 13–23 min (mean: 18 min) per individual.

Black-capped petrels were tracked for 11–255 ± 74.2 d (mean: 102.1 d; median: 108.5 d; Table 2, Fig. S3), resulting in 1021 bird-tracking days. We tallied 4656 PTT locations; 73% of all locations were calculated from 4 (or more) Argos messages (location classes 0–3; Table S1). Of all locations, 37% were accurate to <1500 m and 84% were accurate to <10 km. The maximum error radius for locations of class LC 0 (defined by an error radius >1500 m but with no upper limit) was 216 km (Table S1), but the 95th percentile for this class was 17.5 km. Refitted locations (n = 4142) had a mean (±SE) precision of 5.1 ± 2.5 km for longitude and 4.4 ± 2.4 km for latitude.

3.1. Spatial analysis

We had a sufficient number of locations for 7 individuals to be included in the spatial analysis: 3 dark forms and 4 light forms. All individuals ranged from 28.4–43.0° latitude, with the exception of 2 trips to the vicinity of Hispaniola at the end of the tracking period (i.e. at the onset of the next breeding period) (Table 2, Figs. 2 & S2). These 2 trips occurred outside of the study area, and we did not include them in the spatial analysis. Tracked petrels remained west of 60° W, except for one individual that was last located at approximately 50° W (ID 465). Locations were concentrated along the western wall of the Gulf Stream, over the outer continental shelf of the USA. Petrels were located in the interior of the Stream itself and occupied the eastern wall of the Stream and the Sargasso Sea infrequently. One individual (ID 462) utilized the western half of the Sohm Plains, traveling as far north as the Canadian continental shelf off Banquereau Bank.

Overall, birds of the dark form (core area: 87 344 km^2; home range: 291 794 km^2) occupied a more extensive core area than birds of the light form (core area:

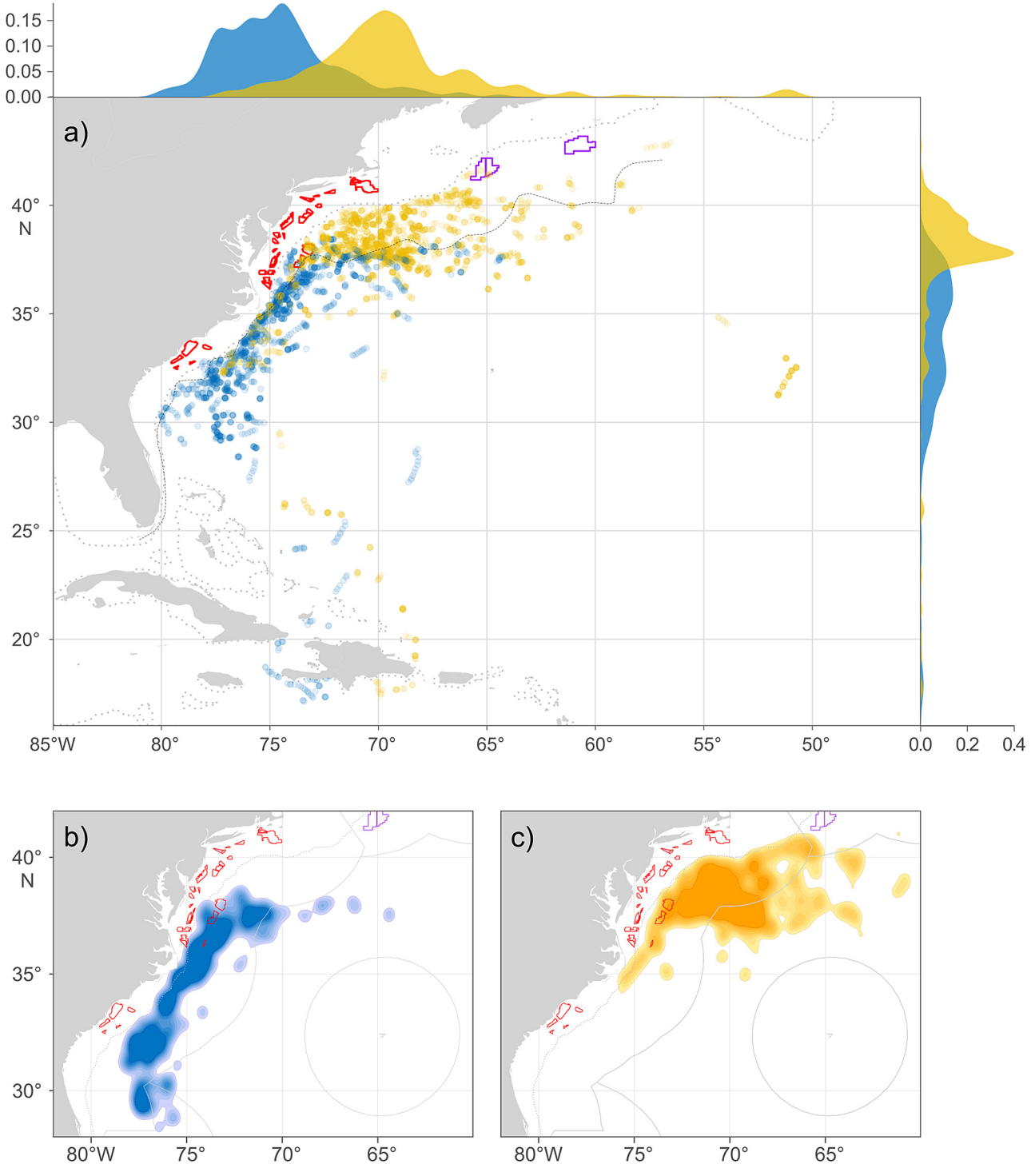

Fig. 2. Distribution of black-capped petrels in the western North Atlantic tracked from (a) May 2019–January 2020 and (b,c) May 2019–August 2019. For all panels, blue represents dark forms and yellow represents light forms. (a) Locations of black-capped petrels (outliers were removed) with frequency distributions of longitude and latitude of dark-form birds and light-form birds overlaid on the top and right border of the panel. (b) Utilization distributions (UDs) of dark black-capped petrels. (c) UDs of light black-capped petrels. For (b) and (c), shading ranges from 50 % UD (darker color) to 90 % UD (lighter color). Dotted grey line: the 250 m isobath; grey polygons: exclusive economic zones; purple polygons: petroleum leases; red polygons: offshore wind leases

Table 3. Summary statistics, significance, and effect size of geographic distributions of black-capped petrels tracked from May 2019–August 2019, grouped by phenotype (n = 3 dark, n = 4 light). p-values and effect sizes are from Wilcoxon rank sum tests. Sample sizes correspond to the number of tracking locations

	Dark (n = 1133)					Light (n = 1771)					p	Effect size
	Median	Mean	Min.	Max.	SD	Median	Mean	Min.	Max.	SD		
Latitude (°N)	35.20	34.50	28.38	38.45	2.73	38.10	38.10	32.29	41.45	1.24	<0.005	1.86
Longitude (°W)	74.60	74.40	78.35	64.27	2.62	69.80	69.60	77.12	60.67	2.82	<0.005	1.78

81 987 km^2; home range: 356 156 km^2) but had a more limited home range. Dark and light forms had significantly distinct distributions (Table 3, Fig. 2). The light form had a narrower and significantly more northerly latitudinal range than the dark form and utilized deeper waters in its core area than the dark form (Table 4, Figs. 2 & S4–S6). In addition, both forms showed extensive longitudinal ranges, with the dark form having a significantly more westerly distribution (Table 3, Fig. 2). The dark morph utilized significantly warmer waters in its core area than the light form in its core area (Table 4, Figs. S5 & S6). Phenotype was a strong predictor of both latitude ($|t|$ = 19.5, $p < 0.005$) and longitude ($|t|$ =18.9, $p < 0.005$)(Table 5).

BAs indicated limited overlap in home ranges (BA = 0.29) and almost no overlap in core areas (BA = 0.03) of dark and light forms. The area of overlap corresponded to 6.0 and 6.4% (50% UD), and 35.4 and 28.9% (90% UD) of the areas used by dark and light forms respectively (Table S2).

Location derived from this tracking study indicated that black-capped petrels occurred in the EEZs of 3 countries plus international waters (Fig. 2, Table S3). US waters accounted for most of the use areas. The proportion of core areas for dark and light forms that occurred in the US EEZ was 99.2 and 74.4% respectively. The proportion of home range areas for dark and light forms that occurred in the US EEZ was 77.4 and 56.2% respectively. The core areas (dark form: 0.8%; light form: 25.6%), and home ranges of both forms (dark form: 15.2%; light form: 41.9%) also overlapped with international waters. The Canadian EEZ was utilized by 1 individual of the light form (home range: 1.9%). The home range of the dark form also overlapped with the Bahamian EEZ (7.4%).

Black-capped petrels occurred in 6 marine ecoregions (including high seas) (Table S4, Fig. S7). The dark form was most present in the Carolinian (50.1% of core area and 39.3% of home range) and Virginian regions (36.7% of core area and 28.3% of home range). The light form was mostly limited to the Virginian region (71.0% of core area and 39.9% of home range) and high seas (29.0% of core area and 47.8% of home range). The dark form made incursions into the high seas (5.8% of core area and 20.8% of home range) and Bahamian region (7.4% of core area and 11.6% of home range). In its home range, the light form seldom utilized the Gulf of Maine/Bay of Fundy (8.6%), Carolinian (3.6%), and Scotian Shelf regions (0.1%).

3.2. Marine threats

Petrels in our study were exposed to mercury concentrations in the 90th quantile of global levels in both their core areas (dark: $\bar{x}_{Hg} = 9.75 \times 10^{-10}$ mol m^{-3}; light: $\bar{x}_{Hg} = 9.44 \times 10^{-10}$ mol m^{-3}) and home ranges (dark: $\bar{x}_{Hg} = 9.55 \times 10^{-10}$ mol m^{-3}; light: $\bar{x}_{Hg} = 9.10 \times 10^{-10}$ mol m^{-3}; 90th quantile: 9.17×10^{-10} mol m^{-3}) (Table 4, Figs. 3 & S5). At the home range level, the dark form was exposed to mercury significantly more than the light form, with a large effect size ($p = 0.001$, $|d| = 0.90$). Differences between forms in the 50% UD, or between UDs within forms, were not significant ($p > 0.05$).

Exposure to microplastics was significantly higher for the dark form compared to the light form at the scale of the entire home range (dark: $\bar{x}_{Plastic} = 247.55$ g km^{-2}; light: $\bar{x}_{Plastic} = 154.92$ g km^{-2}), with a large effect size ($p < 0.005$, $|d| = 0.80$) (Table 4, Figs. 3 & S5). Differences between forms in the 50% UD, or between UDs within forms, were not significant ($p > 0.05$).

Exposure to commercial fishing occurred within 13.0 and 2.6% of the core areas, and 10.5 and 14.0% of the home ranges of dark and light forms, respectively (Table 4, Fig. S5). This exposure occurred in a strip of waters located along the continental shelf from Georges Bank to Hatteras as well as on the continental plateau off the US states of South Carolina and Georgia. In the dark form, average fishing effort equated to 16.8 fishing hours per 0.1° cell in the core area, and 12.4 fishing hours per cell in the home range. Summed fishing effort equated to 1848 fishing hours (50% UD) and 3694 fishing hours (90% UD). In the light form, average fishing effort equated to

Table 4. Characteristics of environmental variables and threat exposure for core area (50% utilization distribution [UD]) and home range (90% UD) of dark and light forms of black-capped petrels tracked from May 2019–August 2019. Sample size (n = number of raster cells in the UD), mean, range, standard deviation, interquartile range (IQR), and p-values of Wilcoxon rank sum tests and Cohen's *d* effect size are provided. For fisheries and ship traffic, proportions of UDs affected, and UD-wide sums of fishing effort and ship counts are provided. SST: sea surface temperature; Hg: mercury. **Bold** lettering denotes significant difference ($p < 0.05$) and moderate or large effects. Effect size: (**) moderate; (***) large

Variable	UD	Dark							Light						p	Effect size
		n	Prop.	Sum	Mean	Min.	Max.	SD	IQR	n	Prop.	Sum	Mean	Min.	Max.	SD	IQR		
Depth (m)	**50**	**265659**	–	–	**–2094.7**	**–4152**	**–6**	**1120.1**	**2103**	**26144**	–	–	**–3418.5**	**–5030**	**–1778**	**670.0**	**1151**	**<0.005**	**1.43*****
	90	**88628**	–	–	**–2637.0**	**–5143**	**–5**	**1485.6**	**2746**	**113485**	–	–	**–3488.9**	**–5417**	**–5**	**1351.2**	**1934**	**<0.005**	**0.60*****
SST (°C)	**50**	**1063**	–	–	**27.4**	**23.8**	**28.6**	**1.11**	**1.34**	**1045**	–	–	**24.4**	**21.5**	**26.9**	**1.47**	**2.81**	**<0.005**	**2.30*****
	90	**3544**	–	–	**26.9**	**22.3**	**28.7**	**1.46**	**1.83**	**4539**	–	–	**24.1**	**14.9**	**28.2**	**2.31**	**3.50**	**<0.005**	**1.40*****
Hg ($\times 10^{-10}$ mol m^{-3})	50	6	–	–	9.75	9.51	9.96	0.16	0.13	7	–	–	9.44	9.00	10.20	0.40	0.40	0.07	0.97***
	90	**28**	–	–	**9.55**	**8.55**	**1.04**	**0.40**	**0.42**	**38**	–	–	**9.10**	**8.03**	**10.20**	**0.56**	**0.81**	**<0.005**	**0.90*****
Plastic (g km^{-2})	50	6	–	–	149.4	86.6	205.8	44.7	59.2	7	–	–	133.0	82.0	198.1	37.9	37.9	0.43	0.40***
	90	**28**	–	–	**247.6**	**85.7**	**730.8**	**152.9**	**154.8**	**38**	–	–	**154.9**	**46.3**	**386.5**	**74.5**	**74.5**	**<0.005**	**0.80*****
Fishing effort (h)	50	113	12.9	1847.9	16.8	0.2	197.2	30.0	15.9	22	2.6	175.7	8.0	0.6	25.1	8.7	10.3	0.62	0.32**
	90	**299**	**10.5**	**3693.8**	**12.4**	**0.2**	**197.2**	**22.3**	**12.7**	**513**	**14.0**	**23503.3**	**45.0**	**0.2**	**1987.1**	**143.9**	**39.3**	**<0.005**	**0.29****
Ship traffic (count)																			
Cargo	**50**	**1260**	**97.3**	**181946**	**144.4**	**0**	**1911**	**259.3**	**113.1**	**1329**	**99.7**	**21789**	**16.4**	**0**	**150**	**15.7**	**14.8**	**<0.005**	**0.71*****
	90	**4152**	**96.4**	**371785**	**89.5**	**0**	**1911**	**201.5**	**60.1**	**5124**	**88.8**	**225780**	**44.1**	**0**	**1911**	**146.3**	**24.1**	**<0.005**	**0.26****
Tanker	**50**	**1234**	**95.3**	**32618**	**26.4**	**0**	**166**	**29.5**	**28.7**	**1252**	**93.9**	**10169**	**8.1**	**0**	**634**	**7.8**	**8.6**	**<0.005**	**0.85*****
	90	**3912**	**90.9**	**69214**	**17.7**	**0**	**195**	**24.3**	**17.8**	**4468**	**77.5**	**56862**	**12.7**	**0**	**166**	**19.8**	**13.4**	**<0.005**	**0.23****
Other	**50**	**1277**	**98.6**	**303318**	**237.5**	**0**	**2701**	**410.0**	**176.6**	**1333**	**100.0**	**37124**	**27.8**	**0**	**235**	**26.1**	**26.7**	**<0.005**	**0.73*****
	90	**4241**	**98.5**	**650004**	**153.3**	**0**	**4194**	**334.9**	**95.8**	**5341**	**92.6**	**430136**	**80.5**	**0**	**2883**	**246.2**	**46.3**	**<0.005**	**0.25****

8.0 fishing hours per 0.1° cell in the core area, and 45.8 fishing hours per cell in the home range. Summed fishing effort equated to 176 fishing hours (50% UD) and 23 503 fishing hours (90% UD). At the home range level, the light form was exposed to fisheries significantly more than the dark, with a moderate effect size ($p < 0.005$, $|d| = 0.29$) (Table 4, Fig. 3).

Although petrels were exposed to shipping activity in most of their core areas and home range (range: 77.5–100.0% of overlap; Table 4, Fig. S5), major shipping routes generally did not overlap with petrel distribution, except for the Chesapeake–Charleston segment in the area of Cape Hatteras. On average in core areas, the dark form was largely more exposed than the light form to cargo ships, tankers, and other types of vessels (Table 4, Fig. S8). On average in home ranges, the dark form was moderately more exposed than the light form to cargo ships, tankers, and other types of vessels (Table 4, Fig. S8).

One black-capped petrel overlapped with active hydrocarbon exploration areas 2435 (n = 3 locations, 6 November) and 2436 (n = 5 locations, 23 and 24 August), in Nova Scotia, Canada (Fig. 2, Table S5). No individuals overlapped with active leases for wind energy. The nearest active wind energy lease area to a petrel location was in North Carolina (29.5 km from location) (Table S5). For wind energy production in the Central Atlantic, 4 individuals overlapped with proposed lease area E-1, 3 with E-2, and one with F-2 (Tables S5 & S6). Three individuals were present in 2 of these proposed leases, and 2 individuals were present in one lease only. In 4 cases, individuals used the same lease area twice, with more than 6 d between visits (mean: 44.8 d between visits, maximum: 98 d). The home range of the dark form slightly overlapped with the active wind lease area in North Carolina (137.3 km^2, 0.05% of the home range). Proposed Central Atlantic wind areas overlapped with core areas (dark: 1.1% of core area; light: 0.9%) and home ranges (dark: 1.1% of home range; light: 1.0%) of both forms (Figs. 2 & S9, Table S6); 14% of the proposed Central Atlantic wind area D was in the home range

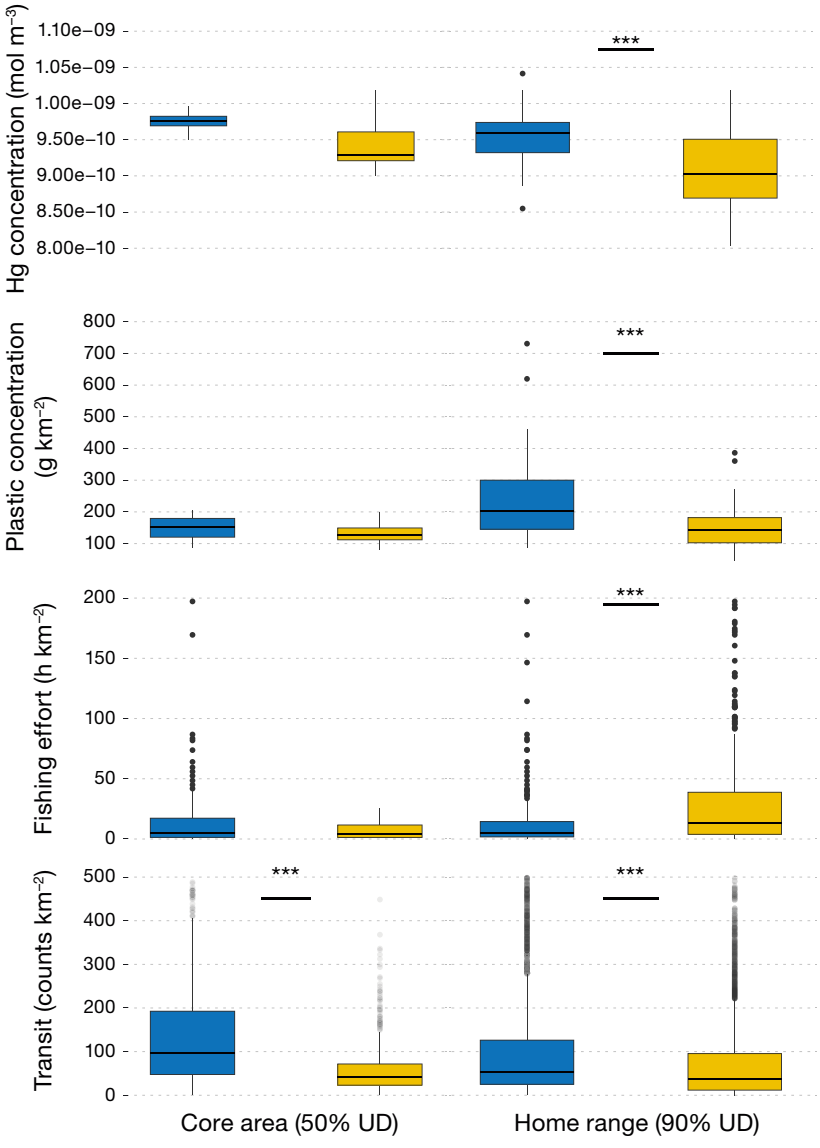

Fig. 3. Distribution of values of threat exposure in the core area and home range of black-capped petrels tracked from May 2019–August 2019. Blue represents dark forms and yellow represents light forms. Solid lines within boxes: median; box edges: quartiles; whiskers extend to 5th and 95th percentiles; circles: data beyond the 95th percentile. ***p < 0.005 (Wilcoxon sum rank test). Note the additional scale for fishing effort in home ranges

Table 5. Characteristics of generalized linear mixed models predicting latitudinal and longitudinal distributions of black-capped petrels tracked from May 2019–August 2019. Models are ordered by rank of prediction of latitude. The best-performing models (Akaike's information criterion ΔAIC < 2) are shown in **bold**

	Latitude			Longitude		
Model	Rank	ΔAIC	Weight	Rank	ΔAIC	Weight
1 + Morph2	**1**	**0.00**	**0.999**	**1**	**0.00**	**0.652**
1+ Morph2 + Sex				**2**	**1.27**	**0.3455**
1 (Intercept)	2	15.98	0.001	3	11.60	0.002
1 + Sex				4	13.31	0.001

of the dark form; 81–100% of E-1, E-2, and F were in the home range of both forms; 59 and 100% of E-2 and F (respectively) were in the core area of the dark form; and 32 and 5% of E-1 and E-2 (respectively) were in the core area of the light form (Table S6, Fig. S9).

4. DISCUSSION

We used tracks from 7 black-capped petrels captured at sea to further enhance our understanding of the spatial distribution of the species in the western North Atlantic. Color forms appeared to differ in their non-breeding distributions and hence their macroscale exposure to marine threats, potentially leading to phenotypically specific ecological niches and differential exposure to ecological drivers of phenotypic divergence (Medrano et al. 2022).

4.1. Marine distribution

More than 5500 at-sea records of black-capped petrels have been confirmed in the US EEZ since 1938 (Sussman & US Geological Survey 2014, Jodice et al. 2021). Together with data from the Caribbean Sea, these records have been used to infer the global range and distribution of the species (Simons et al. 2013, Winship et al. 2018, Leopold et al. 2019, Jodice et al. 2021, Satgé et al. 2023) (Fig. S10). For black-capped petrels, tracking data are limited to the results of 2 studies, each with a sample size of 3 tracked individuals (Jodice et al. 2015, Satgé et al. 2019). Covering a much larger spatial extent than these previous efforts, our study provides a substantial increase in data available to assess the marine distribution of the species. At the species level, our data set showed high overlap with data from at-sea surveys in and around the Hatteras hotspot (i.e. an area similar to the core area of the dark form in our study). Both systematic and

opportunistic at-sea survey data, however, highlighted an area absent from use in our study: the Charleston Bump/Hoyt Hills (Fig. 1). This area, located ~100 km southeast of Charleston, South Carolina, and to the northwest of the Blake Spur has been a historical hotspot for black-capped petrel observations (Haney 1987, eBird 2022) but petrels in our study and in Jodice et al. (2015) showed very limited use of this area, possibly as an artefact of small sample sizes. In contrast, tracking data from the current study showed a much wider use of pelagic waters off the Middle Atlantic Bight and most of the Virginian marine ecoregion compared to at-sea surveys. Most of the population is strongly concentrated in Gulf Stream waters in the Carolinian ecoregion, but petrels in the Virginian region utilized an area of pelagic waters between the northern wall of the Gulf Stream and the continental slope. Finally, except in very limited locations within ca. 100 km of Cape Hatteras, tracked black-capped petrels never occurred on the continental shelf. This is consistent with at-sea surveys in which, except in 2 areas around Cape Hatteras and the Charleston Bump, petrels were only recorded on the continental slope and rise.

By specifically targeting individuals of distinct phenotypes during the capture process, we also were able to test if both phenotypes had similar nonbreeding distributions. Observations from opportunistic surveys (e.g. pelagic birding trips and birding data) suggest that dark-form individuals primarily use central/Carolinian waters and light-form individuals primarily use northern/Virginian waters (eBird 2022), but these records are insufficient for range determination due to their non-systematic nature and inconsistent methodology in reporting the location of observations. Nevertheless, our data set supports this suggestion by showing similar spatial separation in the distributions of the 2 forms. Petrels of the dark form tracked in our study appeared to occupy pelagic Carolinian waters of the South Atlantic Bight and were concentrated within a ~200 km strip of waters extending eastward from the continental shelf into the Gulf Stream. In contrast, light individuals appeared to occupy pelagic Virginian waters of the Middle Atlantic Bight, extending over a wider area between the continental shelf and the northern edge of the Gulf Stream. Consequently, the dark form frequented warm surface waters of the Gulf Stream and, in fact, appears to be one of the seabirds in the western North Atlantic most strongly associated with the Gulf Stream (Winship et al. 2018). In contrast, the light form utilized an area of significantly deeper and colder waters characterized by a wider range of temperatures and more complex oceanic processes compared to the Gulf Stream (Lai & Richardson 1977, Kang & Curchitser 2013). Despite this apparent geographic separation between the 2 forms, light-form petrels remain influenced by the Gulf Stream, whether by latitudinal variability in the path of the Gulf Stream itself or through anticyclonic eddies that diffuse northward (Kang & Curchitser 2013, Seidov et al. 2019). Therefore, the difference in SST that we observed between phenotypes may be more an indication of macroscale differences in habitat availability than active selection of temperate waters by light-form petrels. Indeed, within an overall area of temperate oceanic waters, it is likely that light-form petrels select areas directly influenced by warm oligotrophic waters of anticyclonic eddies (Kang & Curchitser 2013). This selection of eddies has been observed in several species of subtropical and tropical seabirds (e.g. Haney 1986, Hyrenbach et al. 2006, Tew Kai & Marsac 2010). Generally, anticyclonic eddies tend to capture material drifting at the surface (including plankton and fish larvae) and cyclonic eddies tend to expel it to peripheral fronts, hence both potentially increasing prey availability to seabirds at the mesoscale (Cotté et al. 2007). Thus, the more pelagic distribution of the light form may be a response to the lower predictability of anticyclonic eddies (Tew Kai & Marsac 2010) rather than to Gulf Stream fronts, and to a patchier geographic availability of prey across the area (Weimerskirch 2007, Clay et al. 2017).

4.2. Sample size and representativeness of tracked individuals

As is often the case with threatened species or species that use remote areas, the small sample sizes available in our study limit the scope of inference from our results. At the species level, this data set doubles the amount of data available for the black-capped petrel from previous tracking efforts (Jodice et al. 2015, Satgé et al. 2019) and provides detailed information on its marine use in the western North Atlantic. At the phenotype level, the sample size for each form is limited to n = 3 (dark) and n = 4 (light) individuals but may still be sufficient to suggest trends in distributions (Sequeira et al. 2019) or, at a minimum, to develop informed hypotheses for further testing. In general, the home range analysis we used is positively driven by the number of individuals included in calculations, with the area of occupancy increasing with each

new individual and stabilizing around a threshold value (Soanes et al. 2013, Thaxter et al. 2017). In our study, the area of overlap between phenotypes could therefore increase with increased sample size. However, although the observed difference in distributions may be an artefact of the small sample size, the described distributions are in agreement with available pelagic observations (eBird 2022).

Differences in the marine distribution between age groups and/or breeding status may occur within species of pelagic seabirds and therefore could contribute to the dual distribution we observed in our study (e.g. a confounding effect of age or breeding status) (Medrano et al. 2022). For example, juveniles, immatures, and adults may have different spatial or temporal distributions (Péron & Grémillet 2013, Frankish et al. 2020), and failed breeders may have similar or different distributions compared to non-breeders (Phillips et al. 2005, Bogdanova et al. 2011). Petrels utilizing waters off Cape Hatteras in May could be either active breeders (Jodice et al. 2015, Satgé et al. 2019), failed breeders, non-breeders (including skip-breeders, i.e. mature petrels who bred successfully the previous year and skipped breeding in the current year; Hunter et al. 2000, Taylor et al. 2011), or juveniles and immatures (<4 yr of age; Simons et al. 2013). The reproductive status of petrels tracked in this study was not known at the time of capture, and therefore we are unable to accurately assess whether distribution differed by reproductive status. Additionally, except for 2 individuals that were tracked to Hispaniola towards the end of the tracking period during our study (which were likely adults of breeding age), we cannot determine if the petrels were immatures or adults. Nonetheless, we suggest that the dark individuals we captured in May 2019 were unlikely to be adults currently breeding because fledging in the dark form does not occur until after mid-June (Simons et al. 2013, E. Rupp pers. comm.) and chick-rearing petrels appear to remain in the Caribbean Sea and seem less likely to occupy Gulf Stream waters (Jodice et al. 2015). In contrast, previous tracking data indicate that failed breeders vacate the Caribbean and travel to Gulf Stream waters (Jodice et al. 2015). Therefore, we suggest that dark individuals were more likely to be immatures or adults that had skipped breeding or failed at breeding.

The breeding status of light-form birds is more challenging to predict due to limited data from this phenotype. Preliminary data gathered from camera traps from nests of light-form petrels in Valle Nuevo, Dominican Republic, suggest, however, that fledging occurs in late April; hence, our captures may have been post-breeders (E. Rupp pers. comm.). These data, along with the limited extent of the species' distribution in the western North Atlantic and the fact that the dual phenotypic distribution is supported by pelagic observations, suggest that differences in the distribution of immatures, unsuccessful, successful, or non-breeders may be limited in scale in black-capped petrels and that the dual distribution we observed may be driven primarily by phenotype.

Our results also suggest that the dual marine distribution of dark and light forms may be related more to phenotype than date. All individuals were captured within a 25 km radius within 6 d in May 2019. Following captures, most light-form petrels traveled north and stayed in the Virginian ecoregion until the fall, except for one individual that remained in the Carolinian region until June, at which point data transmission ceased. Dark-form petrels remained in the Carolinian region until late July–early August, when they moved to the Virginian region for ca. 1 mo (n = 3). Information is lacking for the remainder of the annual cycle, but the visits to suspected breeding sites on Hispaniola at the end of the tracking period suggest that some degree of tracking nevertheless occurred for most of the non-breeding period. Therefore, although limited by a small sample size, our analysis confirms that phenotypes of the black-capped petrels have distinct non-breeding distributions, independent of the time of the year.

4.3. Exposure to marine threats

Although trait-based approaches are preferred for threat assessments (Butt & Gallagher 2018, Zhou et al. 2019, Richards et al. 2021), substantial data gaps on the biology and ecology of black-capped petrels and uncertainties about the effect of threats, notably marine ones (Wheeler et al. 2021), limit their applicability. Nonetheless, a review of marine threats and likely exposure based on spatial distribution of the species in the western North Atlantic is warranted (Wheeler et al. 2021). Here, we assess exposure at the macro-scale sensu Burger et al. (2011) and Waggitt & Scott (2014); i.e. the occurrence of the species of concern within the geographical area of interest (e.g. the broad area where the threat occurs and overlaps with the species). We assume here that spatial overlap provides an adequate proxy to assess exposure (Michael et al. 2022), with the caveat that overlap at the macroscale likely overestimates actual

overlap at the meso- and microscale (i.e. at finer spatial and temporal scales; Torres et al. 2013). Our limited sample size may negatively affect the calculation of UDs but likely provides an initial, possibly conservative, estimate of potential risk for dark and light forms of the species.

4.3.1. Mercury

Our study shows that petrels were exposed to mercury concentration in the mixed layer in the 90th quantile of global levels. Within the home ranges we calculated, the dark form was significantly more exposed than the light form. Although the mercury model we used fully integrates biogeochemical cycling (Kwon & Selin 2016), it is unclear how well global models like the one by Zhang et al. (2014) capture spatial variation in actual mercury concentrations in the food chain. Nevertheless, our results are consistent with the high levels of total mercury measured in feathers of black-capped petrel (Simons et al. 2013, Y. Satgé unpubl. data, K. Sutherland unpubl. data). Further studies measuring mercury levels in both phenotypes appear warranted to better assess possible repercussions on the meta-population.

4.3.2. Marine plastic

Concentrations of microplastics in black-capped petrel use areas were generally lower than concentrations observed in the study area (Fig. S5). Nevertheless, our data indicate that macro-scale exposure to microplastics was higher in the dark form compared to the light form. The dark form used waters influenced by the southwestern region of the North Atlantic Subtropical Gyre, where the Gulf Stream and Antilles Current converge and where microplastics accumulate (Law et al. 2010, Enders et al. 2015, van Sebille et al. 2015). In contrast, the light form used northern areas where plastic accumulation was limited due to oceanic and atmospheric processes limiting accumulation in the upper oceanic layer (Law et al. 2010). However, the majority of anticyclonic eddies originating from the Gulf Stream are located in the northern areas of the western North Atlantic Ocean, and anticyclonic eddies concentrate microplastics (Brach et al. 2018). Therefore, light-form black-capped petrels may be locally more exposed than dark-form individuals at the meso and micro scale.

4.3.3. Fisheries

Our macro-scale assessment shows limited spatial overlap with fisheries (2.6–13% of core areas and 10.5–14% of home ranges). Relatively high levels of fishing effort (8–17 h cell^{-1} in core areas and 12–46 h cell^{-1} in home ranges) are localized to limited areas on the outer continental shelf. Within our study area, 4 fisheries were responsible for most of the fishing effort in black-capped petrel use areas: demersal trawl, bottom-set longlines, pelagic longlines, and line fishing (Guiet et al. 2019, Global Fishing Watch 2021). Although the relationship between overlap and bycatch is complex and requires information that is currently missing for the black-capped petrel (Wheeler et al. 2021), our results suggest that overlap does exist between endangered black-capped petrels and fisheries in the US EEZ in the western North Atlantic and that data collected at a finer spatial and temporal scale may benefit conservation assessments for the species.

4.3.4. Marine traffic

Given their distribution near major shipping hubs, most, if not all, of the use areas of black-capped petrels are impacted by some level of marine traffic (between 77.5 and 100% of use areas), mostly from cargo ships and other vessels (including fishing vessels). The area of highest overlap was in neritic waters off Cape Hatteras, which is a hotspot of black-capped petrel activity within the core area of the dark form. Our analysis highlights exposure to marine traffic in the US EEZ, but our results are limited by the availability of open-access marine traffic data in the Canadian EEZ (including shipping channels to and from Nova Scotia) and the high seas. Our results should therefore be considered a conservative assessment of black-capped petrel exposure to marine traffic in the western North Atlantic.

4.3.5. Marine energy

There is currently no active petroleum production in the western North Atlantic, but active exploratory leases are present in Canadian waters, and one individual in our study was present in leases 2435 and 2436 (located on Georges Bank). On the US Atlantic coast, there are currently no active oil and gas leases (https://www.boem.gov/oil-gas-energy/oil-and-gas-atlantic; accessed 22 March

2023), but several leases for the production of offshore wind energy are in active states of development in the Middle Atlantic Bight (https://www.boem.gov/renewable-energy/state-activities; accessed 22 March 2023). Because wind energy production is currently logistically constrained to neritic waters, black-capped petrels in our study were not present within active leases. The closest location of a black-capped petrel to an active lease area was ca. 30 km from lease OCS-A 0508 in waters offshore of North Carolina. However, as of late 2022, planning areas have been proposed on the outer continental shelf and rise of the Central Atlantic coast of the USA (Randall et al. 2022) (Fig. 1). These areas overlapped with home ranges and core areas of both phenotypes (Figs. 2 & S9). Therefore, our data suggest that black-capped petrels should be considered for inclusion in ecological assessments and mitigations when future offshore wind energy is developed and produced in these pelagic parts of the western North Atlantic.

5. CONCLUSIONS

Our data suggest that dark and light phenotypes of the black-capped petrel differed in the spatial extent of waters they occupied within the western North Atlantic. The 2 phenotypes may be using different foraging habitats, although the small sample size and coarse scale of our data set prevent detailed modeling of habitat use at this time. Differences in morphology (e.g. bill size) between phenotypes also suggest that dark and light petrels may select different prey and use different foraging strategies, which raises several new questions about the ecological niche and niche partitioning of black-capped petrels at sea. With increased sample size, further research could focus on detailed analyses of habitat selection and elucidate the causes and consequences of this dual distribution between phenotypes. If new breeding areas are discovered for the species, individual-based tracking may be considered to further assess the global connectivity of this endangered species and may identify areas of exposure to anthropic stressors for specific breeding populations (Wheeler et al. 2021).

Data availability. The tracking data set generated during the current study is available in the Movebank data repository (Movebank Study ID 746910348): https://doi.org/10.5441/001/1.0786vv78.

Acknowledgements. We thank Kate Sutherland of Seabirding Pelagic Trips, Hatteras, North Carolina, for help throughout the study. We are grateful to Autumn-Lynn Harrison of the Smithsonian Institute's Migratory Connectivity Project, for generously donating 2 satellite transmitters. We also thank Ari Friedlaender, of the University of California Santa Cruz, for lending us the whale-tagger, and Dive Hatteras in Frisco, North Carolina, for generously providing air tanks. Monica Silva, of Universidade de Lisboa, Portugal, performed the molecular sexing. Zhang Yanxu, of Nanjing University, shared the mercury raster; Erik van Sebille, of Universiteit Utrecht, shared microplastic data sets; and Carina Gjerdrum, of Environment and Climate Change Canada, provided shapefiles of oil and gas leases in Canada. Teresa Militão, Andrew Read, and 2 anonymous reviewers provided helpful reviews that greatly improved the quality of the manuscript. Funding for this research was provided by the Mohamed bin Zayed Species Conservation Fund (project number 12253565), American Bird Conservancy, the South Carolina Cooperative Fish and Wildlife Research Unit, and private donors who contributed to American Bird Conservancy's fundraising campaign. Finally, this study would not have been possible without the trustworthy 'Stormy Petrel II'. The South Carolina Cooperative Fish and Wildlife Research Unit is jointly supported by the US Geological Survey, South Carolina Department of Natural Resources, and Clemson University. Any use of trade, firm, or product names is for descriptive purposes only and does not imply endorsement by the US Government.

LITERATURE CITED

Alerstam T, Bäckman J, Grönroos J, Olofsson P, Strandberg R (2019) Hypotheses and tracking results about the longest migration: the case of the Arctic tern. Ecol Evol 9: 9511–9531

Amante C, Eakins BW (2009) ETOPO1 arc-minute global relief model: procedures, data sources and analysis. NOAA Tech Memo NESDIS NGDC-24

Bernard A, Rodrigues AS, Cazalis V, Grémillet D (2021) Toward a global strategy for seabird tracking. Conserv Lett 14:e12804

BirdLife International (2018) *Pterodroma hasitata*. The IUCN Red List of Threatened Species 2018:e.T22698092A132624510. https://dx.doi.org/10.2305/IUCN.UK.2018-2.RLTS.T22698092A132624510.en (accessed 1 July 2021)

BirdLife International (2023) Species factsheet: *Pterodroma hasitata*. http://datazone.birdlife.org/species/factsheet/black-capped-petrel-pterodroma-hasitata/text (accessed 23 March 2023)

Bogdanova MI, Daunt F, Newell M, Phillips RA, Harris MP, Wanless S (2011) Seasonal interactions in the black-legged kittiwake, *Rissa tridactyla*: links between breeding performance and winter distribution. Proc R Soc B 278:2412–2418

Bond AL, Hobson KA, Branfireun BA (2015) Rapidly increasing methyl mercury in endangered ivory gull (*Pagophila eburnea*) feathers over a 130 year record. Proc R Soc B 282:20150032

Brach L, Deixonne P, Bernard MF, Durand E and others (2018) Anticyclonic eddies increase accumulation of microplastic in the North Atlantic subtropical gyre. Mar Pollut Bull 126:191–196

Bridle JR, Pedro PM, Butlin RK (2004) Habitat fragmentation

and biodiversity: testing for the evolutionary effects of refugia. Evolution 58:1394–1396
Burger J, Gordon C, Lawrence J, Newman J, Forcey G, Vlietstra L (2011) Risk evaluation for federally listed (roseate tern, piping plover) or candidate (red knot) bird species in offshore waters: a first step for managing the potential impacts of wind facility development on the Atlantic Outer Continental Shelf. Renew Energy 36:338–351
Butt N, Gallagher R (2018) Using species traits to guide conservation actions under climate change. Clim Change 151:317–332
Butt N, Halpern BS, O'Hara CC, Allcock AL and others (2022) A trait-based framework for assessing the vulnerability of marine species to human impacts. Ecosphere 13:e3919
Calenge C (2006) The package 'adehabitat' for the R software: a tool for the analysis of space and habitat use by animals. Ecol Modell 197:516–519
Carroll MJ, Wakefield ED, Scragg ES, Owen E and others (2019) Matches and mismatches between seabird distributions estimated from at-sea surveys and concurrent individual-level tracking. Front Ecol Evol 7:333
Clay TA, Phillips RA, Manica A, Jackson HA, Brooke ML (2017) Escaping the oligotrophic gyre? The year-round movements, foraging behaviour and habitat preferences of Murphy's petrels. Mar Ecol Prog Ser 579:139–155
Cohen J (1988) Statistical power analysis for the behavioral sciences, 2nd edn. Lawrence Erlbaum Associates, Hillsdale, NJ
Copsey S (2022) Rarity finders: black-capped petrel in the Canary Islands. https://www.birdguides.com/articles/western-palearctic/rarity-finders-black-capped-petrel-in-the-canary-islands/ (accessed 22 March 2023)
Cotté C, Park YH, Guinet C, Bost CA (2007) Movements of foraging king penguins through marine mesoscale eddies. Proc R Soc B 274:2385–2391
Croxall JP, Silk JR, Phillips RA, Afanasyev V, Briggs DR (2005) Global circumnavigations: tracking year-round ranges of nonbreeding albatrosses. Science 307:249–250
Cummings JA, Smedstad OM (2013) Variational data assimilation for the global ocean. In: Park S, Xu L (eds) Data assimilation for atmospheric, oceanic and hydrologic applications, Vol 2. Springer, Berlin, p 303–343
Danckwerts DK, Humeau L, Pinet P, McQuaid CD, Le Corre M (2021) Extreme philopatry and genetic diversification at unprecedented scales in a seabird. Sci Rep 11:6834
Debski I, Pierre J (2014) Seabird cryptic mortality and risk from fisheries. In: Second meeting of the Scientific Committee of the South Pacific Regional Fisheries Management Organization, 1–7 October 2014, Honolulu, HI
Dias MP, Martin R, Pearmain EJ, Burfield IJ and others (2019) Threats to seabirds: a global assessment. Biol Conserv 237:525–537
eBird (2022) eBird: an online database of bird distribution and abundance. Cornell Lab of Ornithology, Ithaca, NY. www.ebird.org (accessed 1 September 2022)
Enders K, Lenz R, Stedmon CA, Nielsen TG (2015) Abundance, size and polymer composition of marine microplastics ≥10 µm in the Atlantic Ocean and their modelled vertical distribution. Mar Pollut Bull 100:70–81
Ennos RA, French GC, Hollingsworth PM (2005) Conserving taxonomic complexity. Trends Ecol Evol 20:164–168
Fieberg J, Kochanny CO (2005) Quantifying home-range overlap: the importance of the utilization distribution. J Wildl Manag 69:1346–1359
Fischer JH, Debski I, Spitz DB, Taylor GA, Wittmer HU (2021) Year-round offshore distribution, behaviour, and overlap with commercial fisheries of a Critically Endangered small petrel. Mar Ecol Prog Ser 660:171–187
Fox CH, O'Hara PD, Bertazzon S, Morgan K, Underwood FE, Paquet PC (2016) A preliminary spatial assessment of risk: marine birds and chronic oil pollution on Canada's Pacific coast. Sci Total Environ 573:799–809
Frankish CK, Phillips RA, Clay TA, Somveille M, Manica A (2020) Environmental drivers of movement in a threatened seabird: insights from a mechanistic model and implications for conservation. Divers Distrib 26:1315–1329
Fraser GS, Carter AV (2018) Seabird attraction to artificial light in Newfoundland and Labrador's offshore oil fields: documenting failed regulatory governance. Ocean Yearb Online 32:265–282
Fraser GS, Russell J, Von Zharen W (2006) Produced water from offshore oil and gas installations on the Grand Banks, Newfoundland: Are the potential effects to seabirds sufficiently known? Mar Ornithol 34:147–156
Fridolfsson AK, Ellegren H (1999) A simple and universal method for molecular sexing of non-ratite birds. J Avian Biol 30:116
Friesen VL (2015) Speciation in seabirds: Why are there so many species … and why aren't there more? J Ornithol 156:27–39
Furness RW (1985) Ingestion of plastic particles by seabirds at Gough Island, South Atlantic Ocean. Environ Pollut 38:261–272
Gaston AJ (2001) Taxonomy and conservation: thoughts on the latest BirdLife International listings for seabirds. Mar Ornithol 29:1–6
Glass JP, Ryan PG (2013) Reduced seabird night strikes and mortality in the Tristan rock lobster fishery. Afr J Mar Sci 35:589–592
Global Fishing Watch (2021) Fishing effort.
Goutte A, Bustamante P, Barbraud C, Delord K, Weimerskirch H, Chastel O (2014) Demographic responses to mercury exposure in two closely related Antarctic top predators. Ecology 95:1075–1086
Guiet J, Galbraith E, Kroodsma D, Worm B (2019) Seasonal variability in global industrial fishing effort. PLOS ONE 14:e0216819
Haney JC (1986) Seabird segregation at Gulf Stream frontal eddies. Mar Ecol Prog Ser 28:279–285
Haney JC (1987) Aspects of the pelagic ecology and behavior of the black-capped petrel (*Pterodroma hasitata*). Wilson Bull 99:153–312
Hellberg ME (2009) Gene flow and isolation among populations of marine animals. Annu Rev Ecol Evol Syst 40: 291–310
Heubeck M, Camphuysen KCJ, Bao R, Humple D and others (2003) Assessing the impact of major oil spills on seabird populations. Mar Pollut Bull 46:900–902
Howell S, Patteson JB (2008) Variation in the black-capped petrel — One species or more? Alula 14:70–83
Hunter C, Moller H, Fletcher D (2000) Parameter uncertainty and elasticity analyses of a population model: setting research priorities for shearwaters. Ecol Modell 134:299–324
Hyrenbach KD, Veit RR, Weimerskirch H, Hunt GL Jr (2006) Seabird associations with mesoscale eddies: the subtropical Indian Ocean. Mar Ecol Prog Ser 324:271–279
Jodice PGR, Ronconi RA, Rupp E, Wallace GE, Satgé Y (2015) First satellite tracks of the Endangered black-capped petrel. Endang Species Res 29:23–33

Jodice PGR, Michael PE, Gleason JS, Haney JC, Satgé YG (2021) Revising the marine range of the endangered black-capped petrel *Pterodroma hasitata*: occurrence in the northern Gulf of Mexico and exposure to conservation threats. Endang Species Res 46:49–65

Jonsen ID, McMahon CR, Patterson TA, Auger-Méthé M, Harcourt R, Hindell MA, Bestley S (2019) Movement responses to environment: fast inference of variation among southern elephant seals with a mixed effects model. Ecology 100:e02566

Kang D, Curchitser EN (2013) Gulf Stream eddy characteristics in a high-resolution ocean model. J Geophys Res Oceans 118:4474–4487

King MD, Elliott JE, Williams TD (2021) Effects of petroleum exposure on birds: a review. Sci Total Environ 755:142834

Kroodsma DA, Mayorga J, Hochberg T, Miller NA and others (2018) Tracking the global footprint of fisheries. Science 359:904–908

Kuhn M, Wing J, Weston S, Williams A, Keefer C, Engelhardt A (2020) caret: classification and regression training. R package version 6.0-86. https://CRAN.R-project.org/web/packages/caret/

Kwon SY, Selin NE (2016) Uncertainties in atmospheric mercury modeling for policy evaluation. Curr Pollut Rep 2: 103–114

Lai DY, Richardson PL (1977) Distribution and movement of Gulf Stream rings. J Phys Oceanogr 7:670–683

Law KL, Morét-Ferguson S, Maximenko NA, Proskurowski G, Peacock EE, Hafner J, Reddy CM (2010) Plastic accumulation in the North Atlantic Subtropical Gyre. Science 329:1185–1188

Le Bot T, Lescroël A, Grémillet D (2018) A toolkit to study seabird–fishery interactions. ICES J Mar Sci 75:1513–1525

Leopold MF, Geelhoed SC, Scheidat M, Cremer J, Debrot AO, Van Halewijn R (2019) A review of records of the black-capped petrel *Pterodroma hasitata* in the Caribbean Sea. Mar Ornithol 47:235–241

Li Y, Jiao Y, Browder JA (2016) Assessment of seabird bycatch in the US Atlantic pelagic longline fishery, with an extra exploration on modeling spatial variation. ICES J Mar Sci 73:2687–2694

Lieske DJ, Tranquilla LM, Ronconi RA, Abbott S (2020) 'Seas of risk': assessing the threats to colonial-nesting seabirds in Eastern Canada. Mar Policy 115:103863

Lombal AJ, O'dwyer JE, Friesen V, Woehler EJ, Burridge CP (2020) Identifying mechanisms of genetic differentiation among populations in vagile species: historical factors dominate genetic differentiation in seabirds. Biol Rev Camb Philos Soc 95:625–651

Mancilla-Morales MD, Romero-Fernández S, Contreras-Rodríguez A, Flores-Martínez JJ and others (2020) Diverging genetic structure of coexisting populations of the black storm-petrel and the least storm-petrel in the Gulf of California. Trop Conserv Sci 13:1–12

Manly B, Arbogast BS, Lee DS, Tuinen MV (2013) Mitochondrial DNA analysis reveals substantial population structure within the endangered black-capped petrel (*Pterodroma hasitata*). Waterbirds 36:228–233

Medrano F, Militão T, Gomes I, Sardà-Serra M, de la Fuente M, Dinis HA, González-Solís J (2022) Phenological divergence, population connectivity and ecological differentiation in two allochronic seabird populations. Front Mar Sci 9:975716

Michael PE, Hixson KM, Haney JC, Satgé YG, Gleason JS, Jodice PG (2022) Seabird vulnerability to oil: exposure potential, sensitivity, and uncertainty in the northern Gulf of Mexico. Front Mar Sci 9:880750

Moser ML, Lee DS (1992) A fourteen-year survey of plastic ingestion by western North Atlantic seabirds. Colon Waterbirds 15:83–94

Mott R, Clarke RH (2018) Systematic review of geographic biases in the collection of at-sea distribution data for seabirds. Emu 118:235–246

Office for Coastal Management (2021) AIS 2017 vessel transit counts. https://www.fisheries.noaa.gov/inport/item/55365

Parker GC, Rexer-Huber K (2019) Characterisation and mitigation of protected species interactions in inshore trawl fisheries. Report to Conservation Services Programme. Parker Conservation, Dunedin

Pereira JM, Ramos JA, Marques AM, Ceia FR, Krüger L, Votier SC, Paiva VH (2021) Low spatial overlap between foraging shearwaters during the breeding season and industrial fisheries off the west coast of Portugal. Mar Ecol Prog Ser 657:209–221

Péron C, Grémillet D (2013) Tracking through life stages: adult, immature and juvenile autumn migration in a long-lived seabird. PLOS ONE 8:e72713

Phillips RA, Silk JR, Croxall JP, Afanasyev V, Bennett VJ (2005) Summer distribution and migration of nonbreeding albatrosses: individual consistencies and implications for conservation. Ecology 86:2386–2396

R Core Team (2020) R: a language and environment for statistical computing. R Foundation for Statistical Computing, Vienna

Randall AL, Jossart JA, Jensen BM, Duplantis BH, Morris JA (2022) Development of the Central Atlantic wind energy areas. BOEM–NCCOS Joint Report. Bureau of Ocean Energy Management and National Centers for Coastal Ocean Science, Washington, DC

Rayner MJ, Baird KA, Bird J, Cranwell S and others (2020) Land and sea-based observations and first satellite tracking results support a New Ireland breeding site for the Critically Endangered Beck's petrel *Pseudobulweria beckii*. Bird Conserv Int 30:58–74

Rexer-Huber K, Parker GC (2019) Characterising discharge management in small-vessel trawl and longline fisheries. Report to Conservation Services Programme. Parker Conservation, Dunedin

Ribeiro AM, Lloyd P, Feldheim KA, Bowie RCK (2012) Microgeographic socio-genetic structure of an African cooperative breeding passerine revealed: integrating behavioural and genetic data. Mol Ecol 21:662–672

Richard Y, Abraham ER, Berkenbusch K (2017) Assessment of the risk of commercial fisheries to New Zealand seabirds, 2006–07 to 2014–15. Ministry for Primary Industries, Manatū Ahu Matua, Wellington

Richards C, Cooke RS, Bates AE (2021) Biological traits of seabirds predict extinction risk and vulnerability to anthropogenic threats. Glob Ecol Biogeogr 30:973–986

Robinson Willmott J, Forcey G, Kent A (2013) The relative vulnerability of migratory bird species to offshore wind energy projects on the Atlantic Outer Continental Shelf: an assessment method and database. OCS Study BOEM 2013-207. Bureau of Ocean Energy Management, Washington, DC

Rodríguez A, Arcos JM, Bretagnolle V, Dias MP and others (2019) Future directions in conservation research on petrels and shearwaters. Front Mar Sci 6:94

Ronconi RA, Allard KA, Taylor PD (2015) Bird interactions with offshore oil and gas platforms: review of impacts and monitoring techniques. J Environ Manage 147:34–45

Ryan PG, Bourgeois K, Dromzée S, Dilley BJ (2014) The occurrence of two bill morphs of prions *Pachyptila vittata* on Gough Island. Polar Biol 37:727–735

Ryan PG, Ryan EM, Glass JP (2021) Dazzled by the light: the impact of light pollution from ships on seabirds at Tristan da Cunha. Ostrich 92:218–224

Satgé YG, Rupp E, Jodice PGR (2019) A preliminary report of ongoing research of the ecology of black-capped petrel (*Pterodroma hasitata*) in Sierra de Bahoruco, Dominican Republic — I: GPS tracking of breeding adults. South Carolina Cooperative Fish and Wildlife Research Unit, Clemson, SC

Satgé Y, Brown A, Wheeler JA, Sutherland KE (2023) Black-capped petrel (*Pterodroma hasitata*), version 2.0. In: Billeman SM (ed) Birds of the world. Cornell Lab of Ornithology, Ithaca, NY

Sawilowsky SS (2009) New effect size rules of thumb. J Mod Appl Stat Methods 8:597–599

Seidov D, Mishonov A, Reagan J, Parsons R (2019) Resilience of the Gulf Stream path on decadal and longer timescales. Sci Rep 9:11549

Sequeira AM, Heupel M, Lea M, Eguíluz VM and others (2019) The importance of sample size in marine megafauna tagging studies. Ecol Appl 29:e01947

Shaffer SA, Tremblay Y, Weimerskirch H, Scott D and others (2006) Migratory shearwaters integrate oceanic resources across the Pacific Ocean in an endless summer. Proc Natl Acad Sci USA 103:12799–12802

Simons TR, Lee DS, Haney JC (2013) Diablotin *Pterodroma hasitata*: a biography of the endangered black-capped petrel. Mar Ornithol 41:1–43

Soanes LM, Arnould JP, Dodd SG, Sumner MD, Green JA (2013) How many seabirds do we need to track to define home-range area? J Appl Ecol 50:671–679

Spalding MD, Fox HE, Allen GR, Davidson N and others (2007) Marine ecoregions of the world: a bioregionalization of coastal and shelf areas. Bioscience 57:573–583

Sussman A, US Geological Survey (2014) Atlantic offshore seabird dataset catalog, Atlantic coast and outer continental shelf, from 1938-01-01 to 2013-12-31 (NCEI Accession 0115356). Dataset. https://catalog.data.gov/dataset/atlantic-offshore-seabird-dataset-catalog-atlantic-coast-and-outer-continental-shelf-from-1938-1

Tartu S, Goutte A, Bustamante P, Angelier F and others (2013) To breed or not to breed: endocrine response to mercury contamination by an Arctic seabird. Biol Lett 9: 20130317

Taylor GA, Elliott GP, Walker KJ, Bose S (2011) Year-round distribution, breeding cycle, and activity of white-headed petrels (*Pterodroma lessonii*). Notornis 67:369–386

Tew Kai E, Marsac F (2010) Influence of mesoscale eddies on spatial structuring of top predators' communities in the Mozambique Channel. Prog Oceanogr 86:214–223

Thaxter CB, Clark NA, Ross-Smith VH, Conway GJ, Bouten W, Burton NH (2017) Sample size required to characterize area use of tracked seabirds. J Wildl Manag 81: 1098–1109

Torchiano M (2020) effsize: efficient effect size computation. R package version 0.8.1. https://CRAN.R-project.org/package=effsize

Torres LG, Sagar PM, Thompson DR, Phillips RA (2013) Scaling down the analysis of seabird–fishery interactions. Mar Ecol Prog Ser 473:275–289

US Fish and Wildlife Service (2018) Endangered and threatened wildlife and plants; threatened species status for black-capped petrel: 83 FR 50560. Fed Regist 83: 50560–50574

van Sebille E, Wilcox C, Lebreton L, Maximenko N and others (2015) A global inventory of small floating plastic debris. Environ Res Lett 10:124006

VLIZ (Flanders Marine Institute) (2019) Maritime boundaries geodatabase: maritime boundaries and exclusive economic zones (200NM), version 11.

Waggitt JJ, Scott BE (2014) Using a spatial overlap approach to estimate the risk of collisions between deep diving seabirds and tidal stream turbines: a review of potential methods and approaches. Mar Policy 44:90–97

Waugh SM, Filippi DP, Kirby DS, Abraham E, Walker N (2012) Ecological risk assessment for seabird interactions in Western and Central Pacific longline fisheries. Mar Policy 36:933–946

Weimerskirch H (2007) Are seabirds foraging for unpredictable resources? Deep Sea Res II 54:211–223

Wheeler JA, Satgé YG, Brown A, Goetz JE, Keitt BS, Nevins H, Rupp E (2021) Black-capped petrel (*Pterodroma hasitata*) conservation update and action plan: conserving the diablotin. International Black-capped Petrel Conservation Group. https://www.birdscaribbean.org/wp-content/uploads/2021/10/2021-Black-capped-Petrel-Conservation-Update-and-Plan.pdf

Winker K (2010) Subspecies represent geographically partitioned variation, a gold mine of evolutionary biology, and a challenge for conservation. Ornithol Monogr 67: 6–23

Winship AJ, Kinlan BP, White TP, Leirness J, Christensen J (2018) Modeling at-sea density of marine birds to support Atlantic marine renewable energy planning: final report. US Department of the Interior, Bureau of Ocean Energy Management, Office of Renewable Energy Programs, Sterling, VA

Zhang Y, Jaeglé L, Thompson L, Streets DG (2014) Six centuries of changing oceanic mercury. Global Biogeochem Cycles 28:1251–1261

Zhou C, Jiao Y, Browder J (2019) Seabird bycatch vulnerability to pelagic longline fisheries: ecological traits matter. Aquat Conserv 29:1324–1335

Editorial responsibility: Rebecca Lewison, San Diego, California, USA
Reviewed by: F. Medrano and 1 anonymous referee

Submitted: December 12, 2022
Accepted: May 8, 2023
Proofs received from author(s): June 27, 2023